

Atmospheric correction algorithms for satellite ocean color data: performance comparison of “OCTS-type” and “CZCS-type” algorithms

Hajime Fukushima*, Yasushi Mitomi, Takashi Otake*, and Mitsuhiro Toratani***

School of High-Tech., Tokai University*, Remote Sensing Technology Center**

위성해색자료의 대기보정 알고리즘 : OCTS-type과 CZCS-type 알고리즘의 성능비교

하지메 후쿠시마* · 야수시 미토미 · 타카시 오타케* · 미수히로 토라타니***

도카이대학 첨단기술과*, 원격탐사 기술센터**

Abstract

The paper first describes the atmospheric correction algorithm for the Ocean Color and Temperature Scanner (OCTS) visible band data used at Earth Observation Center (EOC) of National Space Development Agency of Japan (NASDA). It uses 10 candidate aerosol models including “Asian dust model” introduced in consideration of the unique feature of aerosols over the east Asian waters. Based on the observations at 670 and 865 nm bands where the reflectance of the water body can be discarded, the algorithm selects a pair of aerosol models that accounts best for the observed spectral reflectances to synthesize the aerosol reflectance in other bands. The paper also evaluates the performance of the algorithm by comparing the satellite estimates of water-leaving radiance and chlorophyll-a concentration with selected buoy- and ship-measured data. In comparison with the old CZCS-type atmospheric correction algorithm where the aerosol reflectance is assumed to be spectrally independent, the OCTS algorithm records factor 2-3 less error in estimating the normalized water-leaving radiances. In terms of chlorophyll-a concentration estimation, however, the accuracy stays very similar compared to that of the CZCS-type algorithm. This is considered to be due to the nature of in-water algorithm which relies on spectral ratio of water-leaving radiances.

요 약

본 논문에서는 우선 NASADA의 지구관측센터에서 활용하는 OCTS 가시광밴드 자료의 대기보정 알고리즘에 대하여 설명하고자 한다. 이 알고리즘은 동아시아 해역 에어로솔의 특징이 고려된 Asian Dust Model을 포함한 10개의 후보 에어로솔 모델을 사용한다. 해수면의 반사율이 제거될 수 있는 670 nm와 865 nm 밴드의 관측에 기초하여, 알고리즘은 다른 밴드에서의 에어로솔 반사율을 합성하기 위한 관측 스펙트럼 반사율을 가장 잘 설명하는 한쌍의 에어로솔 모델을 선택한다. 또한 본 논문에서는 해수에서 나오는 방사량의 위성측정치와 선택된 부표 주위에 집중된 Chlorophyll, 그리고 선성측정 자료를 비교함으로써 알고리즘의 성능을 평가한다. 스펙트럼으로 에어로솔의 반사율이 독립적으로 추정되는 예전의 CZCS-type 대기보정 알고리즘과 비교하여 볼 때, OCTS 알고리즘은 표준화 된 해수에서 나오는 방사량을 측정할 때 Factor 2-3 정도 더 적은 오차를 기록한다. 그렇지만 농도추정 Chlorophyll의 관점에서 보면 정확도가 예전의 CZCS-type 알고리즘과 비교하여 매우 비슷하게 유지된다. 이것은 해수에서 나오는 방사량의 스펙트럼비율에 따르는 해수내의 (in-water) 알고리즘 성질 때문이라고 사료된다.

1. Introduction

In regard with the atmospheric correction of the data acquired by Coastal Zone Color Scanner (CZCS) which had been operated 1978-1986 aboard Nimbus-7 satellite, Gordon *et al.* (1983) proposed an algorithm based on the single scattering approximation for the atmospheric scattering light. The algorithm uses a simple model on the spectral ratio of the aerosol optical thickness called Ångström's law. Due to the limited number of CZCS observation bands, there is not enough information to infer spectral dependency of aerosol reflectance on pixel by pixel basis, and they assumed that the value of ϵ , a parameter that controls the spectral dependency, remains constant throughout an entire CZCS scene with the size of 800 Km (along track) by 1500 Km (cross track). Nevertheless, the algorithm was widely accepted (see Feldman *et al.*, 1989, for example) and provided us with satisfiable result for most of the cases.

For Ocean Color and Temperature Scanner (OCTS) and Sea Wide Field-of-view Scanner (SeaWiFS), much improvement in the performance is endeavored because these instruments observe the ocean surface over factor-2 wide spectral range (412 ~ 865nm) with higher radiometric resolution (10 bits). Gordon and Wang (1994) proposed an algorithm for SeaWiFS data that takes the following elements, (a) pixel-wise aerosol-type variability, and (b) multiple scattering that involves aerosol, into account. The atmospheric correction algorithm used since April, 1997 at Earth Observation Center (EOC) of National Space Development Agency of Japan (NASDA) for the OCTS standard data products is based on that algorithm with some modifications.

In this paper, we first describe the OCTS algorithm that uses ten aerosol models including that of Asian dust. In the same way as the Gordon and Wangs algorithm, it selects an appropriate pair of aerosol models that accounts best for the observed aerosol radiances in two near-infrared (NIR) bands and determines the interpolation ratio between the aerosol reflectances of the two models. In order to validate our algorithm, we compare satellite estimates of the water-leaving radiance and concentration with the selected ship/buoy measurements. The performance of the CZCS-type algorithm is also evaluated in the same way as for the current OCTS algorithm.

2. OCTS Atmospheric Correction Algorithm

OCTS aboard ADEOS satellite had been routinely operated since November 1st, 1996 to June 30, 1997, collecting global ocean color data that amounts far more than the CZCS data set. The instrument has 8 observation bands centered at 412, 443, 490, 520, 565, 670, 765, and 865 nm. The nominal bandwidths for 412-670 nm bands are 20 nm while 765 and 865 nm bands have 40 nm width. For more detailed specification, see Shimada *et al.* (submitted).

The current OCTS algorithm is based on the SeaWiFS algorithm (Gordon and Wang, 1994) but differs from it mainly in the following aspects.

- (a) OCTS algorithm uses a table that relates aerosol reflectance $\rho_A + \rho_{MA}$ (multiple scattering included) to aerosol optical thickness, while the SeaWiFS algorithm uses a different table that relates $\rho_A + \rho_{MA}$ to ρ_{AS} , the aerosol reflectance under the single scattering approximation.
- (b) It determines two candidate aerosol models and the interpolation ratio based on the spectral ratio of the aerosol optical thickness rather than ε , or the ratio of single scattering reflectance.
- (c) It uses 670 and 865 nm bands for atmospheric correction while the SeaWiFS project uses 765 and 865 nm bands. The reason for our not choosing 765 nm band is the anticipated difficulty in O_2 absorption correction for that band.

1) Radiative Transfer Model

In what follows, we describe the current OCTS atmospheric correction algorithm briefly. For precise description, see Fukushima *et al.* (in press) and NASDA/EOC (1997).

We assume that the following model equation holds for the satellite-observed radiance ρ_T for each pixel and for each observation band.

$$\rho_T(\lambda) = \rho_M(\lambda) + \rho_A(\lambda) + \rho_{MA}(\lambda) + t(\lambda)\rho_w(\lambda) \quad \dots\dots\dots (1)$$

where λ is wavelength, ρ_M is the reflectance that would be observed from space when the atmosphere consists of gas molecules only, ρ_A is the reflectance that would be observed when the atmosphere comprises aerosol particles only, ρ_{MA} is the reflectance due to the interaction between molecules and aerosol particles, ρ_w is the reflectance of the ocean due to the back-scattering light that emerges from the water body, and t is the transmittance between ocean surface and the satellite. Note that the model equation here is expressed in terms of reflectance rather than radiance, although radiance L and reflectance ρ is easily converted with each other by the following relation.

$$\rho(\lambda) = \frac{\pi L(\lambda)}{F_0'(\lambda)\cos\theta_0} \quad \dots\dots\dots (2)$$

where F_0' is extraterrestrial solar irradiance that takes two times of ozone absorption into account, and θ_0 is the solar zenith angle for that pixel. The transmittance is defined as a product of molecular, ozone, and aerosol transmittances as

$$\begin{aligned} t(\lambda) &= t_M(\lambda) t_{OZ}(\lambda) t_A(\lambda), \\ t_M(\lambda) &= \exp\{-\tau_M(\lambda)/2\cos\theta\}, \quad \dots\dots\dots (3) \\ t_{OZ}(\lambda) &= \exp\{-t_{OZ}(\lambda)/\cos\theta\}, \end{aligned}$$

and

$$t_A(\lambda) = \exp[-\{1-\omega_A(\lambda)\eta(\lambda)\}\tau_A/\cos\theta]$$

where θ is the satellite zenith angle, τ_M , τ_{OZ} , and τ_A are optical thickness of gas molecules, ozone, aerosol, respectively, ω_A is the aerosol single scattering albedo, and η is the forward scattering probability of aerosol. Note that t_M is diffuse transmittance and $\tau_M/2$ is applied instead of τ_M .

It is interesting to compare the model equation (1) with that of the CZCS algorithm, which is expressed as follows (Gordon, 1997).

$$\rho_r(\lambda) = \rho_M(\lambda) + \rho_{AS}(\lambda) + t(\lambda)\rho_w(\lambda) \quad \dots\dots\dots (4)$$

where ρ_{AS} , aerosol single scattering reflectance, is defined by

$$\rho_{AS}(\lambda) = \frac{\omega_A(\lambda)\rho_A(\psi, \lambda)\tau_A(\lambda)}{4\cos\theta_0 \cos\theta} \quad \dots\dots\dots (5)$$

Here, ρ_A is the aerosol scattering phase the function, ψ is the scattering angle, and θ_0 is the

solar zenith angle for the pixel in consideration.

2) Principle of the Algorithm

The purpose of the atmospheric correction is to retrieve the water-leaving reflectance $\rho_w(\lambda)$ from given observed radiance $\rho_T(\lambda)$ for each pixel (see Eq. (1)). Knowing τ_M (which is derived from the surface pressure of the objective analysis data provided by Japan Meteorological Agency) and τ_{OZ} (derived by Total Ozone Mapping System (TOMS) aboard ADEOS), we can calculate the Rayleigh reflectance ρ_M with sufficiently good accuracy. The transmittance t is also calculated with good accuracy in use of τ_A , the aerosol optical thickness, which is estimated during the atmospheric correction, in addition to τ_M and τ_{OZ} . Thus, the only unknown term in Eq. (1) is $\rho_A + \rho_{MA}$. Like the CZCS algorithm, the general idea to do atmospheric correction is to estimate the magnitudes of $\rho_A + \rho_{MA}$ in the shorter wavelength region from $\rho_A + \rho_{MA}$ in the NIR bands (670 ~ 865nm), where ρ_w , the water-leaving radiance is generally very low and can be discarded. That is, we get $\rho_A + \rho_{MA}$ by

$$\rho_A(\lambda) + \rho_{MA}(\lambda) = \rho_T(\lambda) - \rho_M(\lambda) \dots\dots\dots (6)$$

Estimating $\rho_A + \rho_{MA}$ for band 1~5 (412 ~ 565 nm bands) is not straight forward since the spectral relation of $\rho_A + \rho_{MA}$ over the whole visible and NIR region is dependent on θ_0 , θ , and $\Delta\phi$, the relative azimuth angle between the sun and the satellite. Similar to the method proposed by Gordon and Wang (1994), we introduce a table that stores the relation between the aerosol reflectance $\rho_A + \rho_{MA}$ and aerosol optical thickness τ_A for each band, and uses that table to determine the magnitude of $\rho_A + \rho_{MA}$ in the shorter wavelengths based on the estimated spectral ratio of τ_A between the two NIR bands. Specifically, since the relation between $\rho_A + \rho_{MA}$ and τ_A is also dependent on the aerosol type, the table is made to account for a set of aerosol models we assume for our algorithm. We call this table "aerosol reflectance vs. optical thickness table".

Although the precise pixel-wise procedure of atmospheric correction is described later, the general used to "synthesize" the $\rho_A + \rho_{MA}$ in each band. This brings us ρ_w , concluding the atmospheric correction.

Selecting "two" aerosol models is rationalized as follows. We assume that the aerosol type varies continuously over the whole satellite image. If we are to assume only one model for each pixel in consideration, we will get discontinuity in the retrieved images of geophysical value due to the switching over aerosol models. To avoid this, we need a certain kind of averaging or interpolation over limited number of aerosol models. We decided to take a pair to estimate the aerosol reflectance in the visible bands by interpolating the predicted values given by the two

models.

3) Aerosol Models

In regard with the dependency of aerosol optical properties on the type of aerosol, we prepared a set of 10 candidate aerosol models for the OCTS atmospheric correction, whose base models, together with their size parameters are shown in Table 1. All the base models except the Asian dust model are defined the same as the ones proposed by Gordon and Wang (1994) for the SeaWiFS algorithm. The tropospheric model is rural background aerosol and is described in Shettle and Fenn (1979). The maritime and the coastal models are also based on the maritime model defined in the same literature, with different mixture ratio between the rural aerosol and the flow to estimate $\rho_A + \rho_{MA}$ in shorter wavelength region is summarized as follows. First, based on the observed $\rho_A + \rho_{MA}$ in 670 and 865 nm bands, we assume each of aerosol models to estimate τ_A for these bands in use of the aerosol reflectance-optical thickness table. Then, we select a pair of aerosol and, in use of the table again, estimate $\rho_A + \rho_{MA}$ in band 1~5 for each model, which is oceanic aerosol models (99% particles of continental origin for the maritime mode, for example). The coastal model is taken in hope of simulating the aerosol that has more particles of continental origin. The "log-normal" or the "bi-modal log-normal" modeling is used for the size distributions with the standard mode radii r_i and σ_i given in Table 1. That is, the number density $n(r)$ for the radius r is given as follows,

$$n(r) = \sum_{i=1}^2 \left(\frac{N_i}{\sqrt{2\pi} \ln(10) r \sigma_i} \right) \exp \left\{ -\frac{(\log r - \log r_i)^2}{2\sigma_i^2} \right\} \dots\dots\dots (7)$$

Table 1 . Characteristics of the base aerosol models
(Extracted from Shettle and Fenn (1979) with coastal model added)

Aerosol model	Size distribution			Type
	N_i	$r_i(\mu m)$	σ_i	
Tropospheric Coastal	1.0	0.03	0.35	Rural aerosol mixture
Continental origin	0.995	0.03	0.35	Rural aerosol mixture
Oceanic origin	0.005	0.3	0.4	Sea salt solution in water
Maritime				
Continental origin	0.99	0.03	0.35	Rural aerosol mixture
Oceanic origin	0.01	0.3	0.4	Sea salt solution in water

These mode radii corresponds to moderate humidities (70% to 80%)

where \ln means natural logarithm while \log means logarithm with base 10, σ_i is the standard deviation, r_i is the mode radius, and N_i is the number density of i -th component. Note that these radius values in the table are for moderate relative humidities (70 to 80%) and we modified the radii according to Shettle and Fenn (1979). Detailed description is found in Nakajima (1996).

We selected 10 aerosol models to cover the variety of aerosols found over the ocean (Table 2). Models 1 through 9 are the representatives of the three base models with different relative humidities (RH). Model 10, "Asian dust model", is introduced in consideration of the unique feature of local aerosols over the east Asian waters (Fukushima and Toratani, 1997). The size distribution of Asian dust was determined from ground radiometric observations conducted in Nagasaki (Nakajima *et al.*, 1989) while the refractive index was given by S.Ohta (private communication) from the absorption measurement of soil particles sampled at Chinese desert area. Taking account of the nonsphericity of dust particles, semi-empirical parameter tuning introduced by Pollack and Cuzzi (1979) was applied in the Mie calculation (Nakajima, 1996).

To evaluate the extent of the coverage in terms of the spectral dependency of the aerosol reflectance, we have calculated $\varepsilon(\lambda, 865)$ for all the 10 models where $\varepsilon(\lambda, 865)$ is the ratio of aerosol spectral reflectance approximated by single scattering at wavelength λ to that of 865 nm, which is defined as follows.

$$\varepsilon(\lambda, 865) = \frac{\rho_{AS}(\lambda)}{\rho_{AS}(865)} = \frac{\omega_A(\lambda)P_A(\psi, \lambda)\tau_A(\lambda)}{\omega_A(865)P_A(\psi, 865)\tau_A(865)} \dots\dots\dots (8)$$

Table 2. Aerosol models used for OCTS atmospheric correction.

Model No	Description of Aerosol Model
1	Tropospheric model w. R.H. 50 %
2	Tropospheric model w.R.H. 80 %
3	Tropospheric model w.R.H. 90 %
4	Coastal model w.R.H. 50 %
5	Coastal model w.R.H. 80 %
6	Coastal model w.R.H. 90 %
7	Maritime model w.R.H. 50 %
8	Maritime model w.R.H. 80 %
9	Maritime model w.R.H. 99 %
10	Asian dust model

The result shown in the Figure 1 of Fukushima *et al.* (1997) showed that $\varepsilon(\lambda, 865)$ varies as wide as factor 2 or more in the shorter wavelength region.

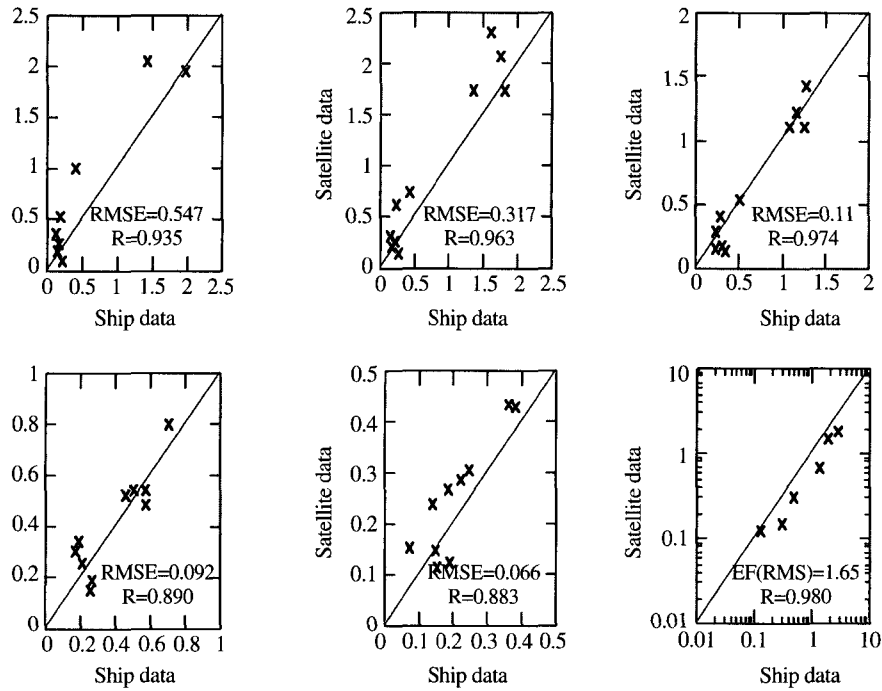


Fig. 1. Comparison of ship-measured and satellite-derived normalized water-leaving radiances and chlorophyll-a concentrations under the "OCTS" atmospheric correction algorithm.

4) Lookup Tables

The actual atmospheric corrections implemented to the data processing system at NASDA/EOC has following lookup tables.

- (1) "Rayleigh reflectance table" which gives $\rho_M(\lambda)$ for given θ , θ_0 , and $\Delta\phi$. The table consists of the Fourier coefficients $c_i(\lambda, \theta, \theta_0)$ ($i=0, 1, 2$) defined as follows, which were calculated for every few degrees.

$$\rho_M(\lambda, \theta, \theta_0, \Delta\phi) = \sum_{i=0}^2 c_i(\lambda, \theta, \theta_0) \cos(m\Delta\phi) \dots\dots\dots (9)$$

where $\Delta\phi$ is the difference between the solar and the satellite azimuth angles.

- (2) "Aerosol reflectance-optical thickness table" for each aerosol model which relates $\rho_A + \rho_{MA}$ to τ_A . After the preliminary analysis, we found that the relation between $\rho_A + \rho_{MA}$ and τ_A can be expressed in cubic polynomial of τ_A with satisfactory accuracy, whose coefficients are determined by the least square method. Thus we decided to have the table consists of coefficients a_1 , a_2 , and a_3 in the equation,

$$\begin{aligned} \rho_A(M, \lambda) + \rho_{MA}(M, \lambda) = & a_1(M, \lambda, \theta, \theta_0, \Delta\phi)\tau_A(M, \lambda) \\ & + a_2(M, \lambda, \theta, \theta_0, \Delta\phi)\tau_A^2(M, \lambda) \dots\dots\dots (10) \\ & + a_3(M, \lambda, \theta, \theta_0, \Delta\phi)\tau_A^3(M, \lambda) \end{aligned}$$

for every few degrees of $(\theta, \theta_0, \Delta\phi)$ for an appropriate set of τ_A values and for every aerosol type M . The values of a_1, a_2, a_3 for given θ, θ_0 , and $\Delta\phi$ are derived from three dimensional Lagrangian interpolation.

- (3) "Single scattering albedo table" which keeps ω_A values for every aerosol model M .
- (4) "Extinction coefficient table" which contains the values of extinction coefficients K_{ext} for every aerosol model M .
- (5) "Phase function table" which retains aerosol scattering phase function $P_A(M, \psi, \lambda)$ for every aerosol model M .

The entries for these tables were all generated by a code for radiative transfer calculation developed by T.Nakajima and his group (Nakajima, 1996). Rayleigh reflectance was calculated with the polarization and the multiple scattering effect taken into consideration, whereas aerosol reflectance was calculated without polarization but with multiple scattering. In both cases we assumed flat specular ocean surface.

5) Procedure of pixel-wise data processing

To select the pair of aerosol models, we define here a parameter γ as

$$\gamma(670,865) = \frac{\tau_A(670)}{\tau_A(865)} \dots\dots\dots (11)$$

We use two kinds of γ in the atmospheric correction process. One is "theoretical" γ , abbreviated as γ_T , defined by

$$\gamma_T(M,670,865) = \frac{K_{ext}(M, 670)}{K_{ext}(M, 865)} \dots\dots\dots (12)$$

where M stands for any one of the 10 aerosol models and K_{ext} stands for the extinction coefficient for the model. Note that τ_A is proportional to K_{ext} . The other is "estimated" γ that is estimated from the satellite measured data. This is abbreviated as γ_E and defined as

$$\gamma_E(M,670,865) = \frac{\tau_A^E(M, 670)}{\tau_A^E(M, 865)} \dots\dots\dots (13)$$

where τ_A^E is the retrieved value of aerosol optical thickness for the assumed aerosol model M . The τ_A^E is obtained by solving the cubic equation (10). For simplicity, we use $\gamma_E(M)$ (or $\gamma_T(M)$)

instead of $\gamma_E(M, 670, 865)$ (or $\gamma_E(M, 670, 865)$) in the following.

Since the γ_T and γ_E values are dependent on the aerosol model, we have 10 γ_T values which are fixed and 10 γ_E values which are variable with pixels. To determine the pair of aerosol models for the pixel in consideration, we calculate a representative value, γ_{AVE} , over the 10 γ_E values, which is hopefully close enough to the more detailed description of the model selection process is shown in the next subsectioning value of the aerosol in the observed area or pixel.

Then, using γ_{AVE} value as an index of the 10 γ_T values, we select 2 models which have the nearest larger or smaller γ_T values compared to γ_{AVE} . The difference between the γ_{AVE} and γ_T values is used to determine the interpolation ratio r that is used to synthesize $\rho_A + \rho_{MA}$ for the 412 ~ 565 nm bands. Namely, the interpolation ratio is defined as

$$\gamma = \frac{\gamma_{AVE} - \gamma_T(M1)}{\gamma_T(M2) - \gamma_T(M1)} \dots\dots\dots (14)$$

where $M1$ and $M2$ are the selected pair of the aerosol models. The pixel-wise procedure of atmospheric correction is described as follows.

[Pixel-wise data processing]

- (1) Estimate τ_A at 670 and 865 nm for each assumed aerosol model(M) by solving the cubic equation (10) in reference to the aerosol reflectance-optical thickness table. Get $\gamma_E(M)$ for each model.
- (2) Get $\rho_A(\lambda) + \rho_{MA}(\lambda) = \rho_T(\lambda) - \rho_M(\lambda)$ at 670 and 865 nm.
- (3) Based on the set of 10 $\gamma_E(M)$ values, calculate γ_{AVE} by one of the three schemes to select a pair of aerosol models $M1$ and $M2$ that have closest $\gamma_T(M)$ values to γ_{AVE} , such that $\gamma_T(M1) < \gamma_{AVE}$ and $\gamma_T(M2) > \gamma_{AVE}$. If γ_{AVE} has higher (or lower) value than all the γ_T values, go to the step (6). Calculate the interpolation ratio r by equation (14).
- (4) For models $M1$ and $M2$, obtain $\tau_A^E(M, \lambda)$ for 412~565 nm bands by
Derive $\rho_A(\lambda) + \rho_{MA}(\lambda)$ for the models $M=M1$ and $M2$ by Eq. (10) in reference to the aerosol reflectance-optical thickness table.

$$\tau_A^E(M, \lambda) = \frac{K_{ext}(M, \lambda)}{K_{ext}(M, 865)} \tau_A^E(M, 865) \dots\dots\dots (15)$$

- (5) Obtain final $\rho_A(M, \lambda) + \rho_{MA}(M, \lambda)$ by interpolating the $\rho_A + \rho_{MA}$ values for the models $M1$ and $M2$. That is,

$$\rho_A(\lambda) + \rho_{MA}(\lambda) = (1-r)\{\rho_A(M1, \lambda) + \rho_{MA}(M1, \lambda)\} + r\{\rho_A(M2, \lambda) + \rho_{MA}(M2, \lambda)\} \dots\dots\dots (16)$$

- (6) (In case γ_{AVE} is higher (or lower) than all the $\gamma_T(M)$ values) Select model 1 (or model 10) to determine $\rho_A(\lambda) + \rho_{MA}(\lambda)$ in the same way as described above but for the single model.

6) Iterative Aerosol Type Selection

We have proposed three different schemes for aerosol type selection and evaluated their performance by numerical simulation (Fukushima *et al.*, 1997). Within the three, a scheme called "weighted average with iteration" showed the best result in terms of the estimation error in the retrieved ρ_w at 443 nm band and was adopted to the so-called version 4 OCTS data processing software used in NASDA/EOC since June, 1998.

Although the precise description of the scheme is rather complicated, the essence of the procedure is to iteratively drop two models to update γ_{AVE} based on new candidate aerosol models. That is, we calculate γ_{AVE} by

$$\gamma_{AVE} = \frac{\sum_C W_M \gamma_E(M)}{\sum_C W_M} \dots\dots\dots (17)$$

where \sum_C means the summation over the current candidate aerosol model set C . At first, C includes all the 10 aerosol models. Then, 2 aerosol models that have largest and second largest $\Delta\gamma(M) = |\gamma_T(M) - \gamma_{AVE}|$ are dropped from C , resulting in new γ_{AVE} . This process is repeated until two final models are selected and the interpolation ratio r is determined.

The rationale for this scheme is that, if an aerosol model is much different from the "true" aerosol model, its theoretical γ value is likely much deviated from γ_{AVE} .

3. Evaluation Of The Algorithm By In-Situ Data

We evaluate here the performance of the OCTS algorithm with the iterative scheme, in comparison with the CZCS algorithm (Gordon *et al.*, 1983) based on the selected ship- or buoy-measured data contributed to the OCTS project at NASDA. The selected data includes those acquired by MOBY moored buoy deployed off Lanai, Hawaii (Clark *et al.*, 1997) and the Yamato Bank Optical Mooring (YBOM) (Kishino *et al.*, 1997). The data were screened so that the ship/buoy observation was conducted within 12 hours from the satellite over-pass under clear sky condition.

$$nL_w(\lambda) = \frac{L_w(\lambda)}{t_0(\lambda)\cos\theta_0} = \frac{F_0(\lambda)\rho_w(\lambda)}{\pi t_0(\lambda)} \dots\dots\dots (18)$$

The OCTS Level-1B data used for the match-up data analysis were provided by the OCTS project at Earth Observation Research Center (EORC) of NASDA. We adopt the gain correction factors that are prepared for NASDA's so-called version 4 data product. After the atmospheric correction was applied, the water-leaving radiance was converted into the normalized water-leaving radiance by the relation,

where t_0 is the transmittance between the sun and the sea surface. The chlorophyll-a concentration (C) was estimated by the following OCTS standard in-water algorithm (Kishino *et al.*, in press).

$$C = 0.2818 \left\{ \frac{nL_W(520) + nL_W(565)}{nL_W(490)} \right\}^{3.49} \dots\dots\dots (19)$$

Figure 1 shows the results of "match-up data analysis" under the OCTS algorithm. Comparisons between satellite-derived and ship-measured normalized water-leaving radiance nL_W for 412~565 nm bands are shown in Figure 1 (a)~(e), where RMSE stands for the root mean square error in radiance ($\mu W/cm^2/sr/nm$) and R stands for the correlation factor. In these figures, there is a tendency that the RMS error increases in the shorter wavelength region, reflecting the increasing difficulty in atmospheric correction for short wavelength bands. Another thing to notice is that the error is generally larger than it should be, considering that the minimum nL_W is about 0.2-0.3 $\mu W/cm^2/sr/nm$ in these bands. Figure 1(f) shows the match-up for chlorophyll-a concentration, indicating that the satellite tends to give lower estimate by a factor of 1.7.

Figure 2 shows the similar results but for the CZCS-type atmospheric correction algorithm that assumes constant ϵ value (we assume $\epsilon(\lambda, 670) = 1.0$) over the whole image, meaning that the algorithm expects constant aerosol type which covers all over the entire image. Very interestingly, while the estimation error in nL_W is about factor 2 to 3 larger than that of the OCTS algorithm, the CZCS algorithm gives as better chlorophyll-a estimates as the OCTS algorithm does. This is considered due to the nature of current chlorophyll-a algorithm that relies on the spectral ratio of water-leaving reflectance.

4. Conclusion

We described our OCTS atmospheric correction algorithm together with three different schemes for the aerosol model selection. Although the OCTS algorithm, in use of the iterative scheme shows satisfiable accuracy in the numerical simulation, the satellite data and *in-situ* measurement comparison suggests that larger errors may be present in the actual data. This may,

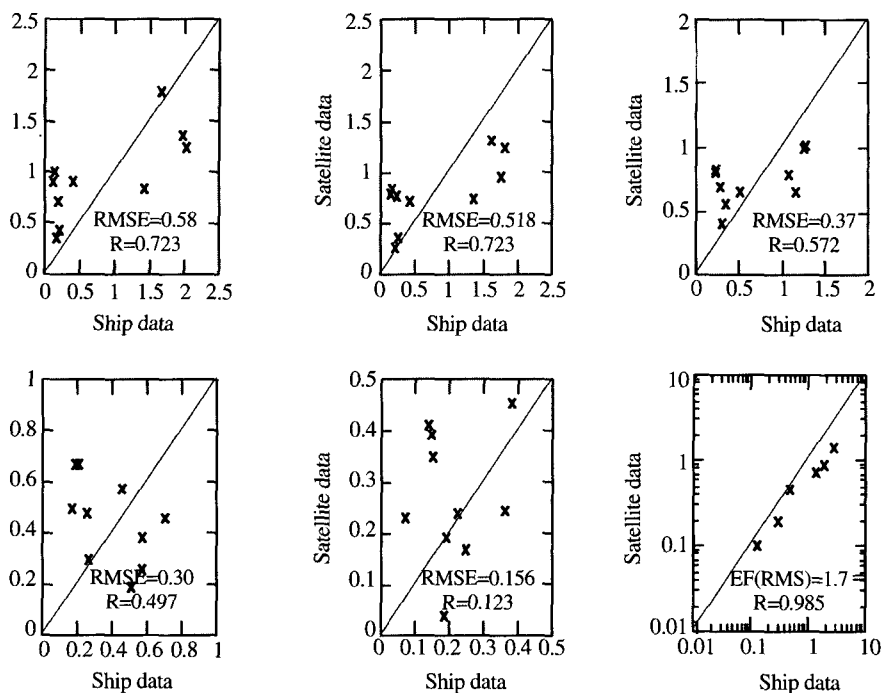


Fig. 2. Comparison of ship-measured and satellite-derived normalized water-leaving radiances and chlorophyll-a concentrations under the CZCS-type atmospheric correction algorithm.

however, be ascribed to the ambiguity of water-leaving radiance measurements conducted by ship or by buoy. Never the less, the authors hope that this study gives a basic idea about the accuracy of the ocean color atmospheric correction. Despite the larger errors in estimating nL , the CZCS algorithm gives as good chlorophyll-a concentration estimates compared to our OCTS algorithm. The CZCS-type algorithm is simple and faster than the OCTS algorithm by a factor of about 5, taking only 30 seconds to do atmospheric correction of 512 by 512 data on Sun UltraSparc 170E workstation. Considering this, one may judge that the CZCS-type algorithm is practically better. It is reminded, however, the future in-water algorithms will surely require the more precise retrieval of nL_w . Hence, we feel that our approach to use a realistic set of aerosol models is along the right direction.

Acknowledgment

The authors thank Dr. T. Nakajima, Dr. A. Higurashi, Mr. T. Tanaka, and W. Takahashi,

who jointly worked for the development and the implementation of the OCTS atmospheric correction algorithm. Special thanks should be extended to the Japanese and the international colleagues who have contributed their in-situ data to NASDA for calibration and validation of OCTS. The support of the OCTS team at NASDA/EORC was also deeply appreciated. This work received support from the National Space Development Agency of Japan (NASDA) under contract PSPC-20117.

Reference

- Clark, D. K., H. R. Gordon, K. J. Voss, Y. Ge, W. Broenkow, and C. Trees, Variation of atmospheric correction over the ocean, *J. Geophys. Res.*, 102, D14, 17209-17217 (1997).
- Feldman, G. C., N. Kuring, C. Ng, W. Esaias, C. McClain, J. Elrod, N. Maynard, D. Endres, R. Evans, J. Brown, S. Walsh, M. Carle, and G. Podesta, Ocean color: availability of the global data set, *Eos Trans. AGU*, 70(23), 634-635, 640-641 (1989).
- Fukushima, H., and M. Toratani, Asian dust aerosol: optical effect on satellite ocean color signal and a scheme of its correction, *J. Geophys. Res.*, 102 (D14), 17, 119-17, 130 (1997)
- Fukushima, H., T. Nogulchi, H. Tabata, and M. Toratani, Evaluation of OCTS atmospheric correction and possible improvement, *Proc. Int. Sym. on Remote Sensing*, Korean Soc. Remote Sensing, 262-268 (1997).
- Fukushima, H., A. Higurashi, Y. Mitomi, T. Nakajima, T. Noguchi, T. Tanaka, and M. Toratani, Correction of atmospheric effect of ADEOS/OCTS ocean color data: Algorithm description and evaluation of its performance, *J. Oceanogr.* (in press).
- Gordon, H.R., D. K. Clark, J. W. Brown, O. B. Brown, R. H. Evans, and W. W. Broenkow., Phytoplankton pigment concentrations in the Middle Atlantic Bight: comparison of ship determinations and CZCS estimates, *Appl. Opt.*, 22(1), 20-36 (1983).
- Gordon, H.R., and M. Wang., Retrieval of water-leaving radiance and aerosol optical thickness over the oceans with SeaWiFS: a preliminary algorithm, *Appl. Opt.*, 33(3), 443-452 (1994).
- Gordon, H. R., Atmospheric correction of ocean color imagery in the Earth observing system era, *J. Geophys. Res.*, 102, D14, 17, 081-17, 106 (1997).
- Kishino, M., J. Ishizaka, S. Saitoh, Y. Senga, and M. Utashima, Verification plan of ocean color and temperature scanner atmospheric correction and phytoplankton pigment by moored optical buoy system, *J. Geophys. Res.*, 102 (D14), 17, 197-17, 207 (1997)
- Kishino, M., T. Ishimaru, K. Furuya, T. Oishi, and K. Kawasaki, In-water algorithms for Ocean Color and Temperature Scanner (OCTS) onboard ADEOS, *J. Oceanogr.* (in press)

- Nakajima, T., M. Tanaka, M. Yamamoto, M. Shiobara, K. Arao, and Y. Nakanishi, Aerosol optical characteristics in the yellow sand events observed in May, 1982 at Nagasaki - part II models, *J. Meteor. Soc. Japan*, 67, 279-291 (1989).
- Nakajima, T, Development of radiance tables for aerosol remote sensing, NASDA's annual report for OCTS project, 43pp. (1996, in Japanese)
- NASDA/EOC, Advanced Earth Observing Satellite (ADEOS): OCTS Data Processing Algorithm Description, Ver. 2.0.1, 1997, Anonymous FTP site, <ftp://ftp2.eorc.nasda.go.jp/pub/format/OCTS/PDF/ALGORITHM/> (1997).
- Pollack, J. B., and J. N. Cuzzi. Scattering by nonspherical particles of size comparable to a wavelength: a new semi-empirical theory and its application to tropospheric aerosols, *J. Atmos. Sci.*, 37, 868-881 (1979).
- Shettle, E. P., and R. W. Fenn, Models for the aerosols of the lower atmosphere and the effects of humidity variations on their optical properties, *AFGL-TR-79-0214*, 675, 94pp (1979).
- Shimada, M., H. Oaku., Y. Mitomi., and H. Murakami, Calibration of the ocean color and temperature scanner, submitted to *IEEE Trans. Geosci. Remote Sensing*.